

## Research Article

# Preparation, Characterization, and Evaluation of Rutin Nanocrystals as an Anticancer Agent against Head and Neck Squamous Cell Carcinoma Cell Line

Sepideh Bohlouli <sup>1</sup>, Faezeh Jafarmadar Gharehbagh <sup>2</sup>, Elaheh Dalir Abdolahinia <sup>3</sup>,  
Maryam Kouhsoltani <sup>4</sup>, Ghasem Ebrahimi <sup>5</sup>, Leila Roshangar <sup>6</sup>, Amir Imani <sup>1</sup>,  
Simin Sharifi <sup>7</sup> and Solmaz Maleki Dizaj <sup>7,8</sup>

<sup>1</sup>Department of Oral Medicine, Faculty of Dentistry, Tabriz University of Medical Sciences, Tabriz, Iran

<sup>2</sup>Immunology Research Center, Tabriz University of Medical Sciences, Tabriz, Iran

<sup>3</sup>Research Center for Pharmaceutical Nanotechnology (RCPN), Tabriz University of Medical Sciences, Tabriz, Iran

<sup>4</sup>Oral and Maxillofacial Department of Pathology, Faculty of Dentistry, Tabriz University of Medical Sciences, Tabriz, Iran

<sup>5</sup>Department of Biochemistry and Clinical Laboratories, Faculty of Medicine, Tabriz University of Medical Sciences, Tabriz, Iran

<sup>6</sup>Stem Cell Research Center, Tabriz University of Medical Sciences, Tabriz, Iran

<sup>7</sup>Dental and Periodontal Research Center, Tabriz University of Medical Sciences, Tabriz, Iran

<sup>8</sup>Department of Dental Biomaterials, Faculty of Dentistry, Tabriz University of Medical Sciences, Tabriz, Iran

Correspondence should be addressed to Simin Sharifi; [sharifi.ghazi@gmail.com](mailto:sharifi.ghazi@gmail.com) and Solmaz Maleki Dizaj; [maleki.s.89@gmail.com](mailto:maleki.s.89@gmail.com)

Received 4 April 2021; Revised 14 August 2021; Accepted 25 August 2021; Published 1 October 2021

Academic Editor: Donglu Shi

Copyright © 2021 Sepideh Bohlouli et al. This is an open access article distributed under the Creative Commons Attribution License, which permits unrestricted use, distribution, and reproduction in any medium, provided the original work is properly cited.

The reports show that rutin has good potentials as an anticancer agent; however, rutin has poor bioavailability due to its low aqueous solubility. The present study was aimed at preparing and evaluating physicochemical properties as well as the anticancer activities of rutin nanocrystals (RNs). RNs were prepared via the ultrasonication method. The prepared nanocrystals then were physicochemically characterized by the conventional techniques. The cytotoxic effect of RNs and free rutin on the HN5 head and neck squamous carcinoma cell line was assessed. The HGF1-PII cells as normal oral cells were treated by RNs. Cells were also exposed to rutin and RNs to determine their effects on the expression of *caspase-8*, *caspase-9*, *Bcl-2*, and *Bax* genes. The prepared RNs have a mean particle size of  $75 \pm 0.16$  nm and quasispherical morphology. Rutin displayed no significant cytotoxic effect on HN5 cells to  $2000 \mu\text{M}$ . However, RNs displayed a cytotoxic effect with  $\text{IC}_{50}$  of  $30.51 \mu\text{M}$  and  $27.34 \mu\text{M}$  in 24 and 48 h incubation times, respectively ( $p < 0.05$ ). RNs had cytotoxic effect 100 times more than rutin on HN5 cells. There was no significant cytotoxic effect on HGF1-PII treated by RNs in 24 and 48 h. The expression of *Bcl-2* mRNA was significantly decreased in attendance of RNs compared to the control group ( $p < 0.05$ ). The increase in *Bax/Bcl-2* ratio was revealed within  $\text{IC}_{50}$  of RNs in 24 h. Our results confirm that the anticancer effect of RNs is significantly more than that of rutin. The activation of the mitochondria-dependent apoptotic pathway of RNs occurred via modulation of *Bcl-2* and *Bax* expression. These results suggest that RNs may be useful in the development of a cancer therapy protocol.

## 1. Introduction

One of the subgroups of oral and oropharyngeal squamous cell carcinomas (SCCs) is oral squamous cell carcinoma (OSCC), which ranks the 11<sup>th</sup> most common

carcinoma in humans. It accounts for 94% of oral cancers and 2-3% of all cancers. It is characterized by the low survival rate and poor prognosis. Despite current developments in the OSCC treatment in the past few decades, the survival rate of patients has only slightly increased;

thus, based on these reasons, it is difficult to overcome OSCC [1–5].

The importance and efficiency of herbs for the treatment of tumors have currently attracted considerable attention worldwide [6–10]. In this regard, flavonoids can be considered as ubiquitous compounds of herbs. These plants have attracted a lot of attention themselves since they have significant impacts on humans' health; reports show their function against viruses, allergies, inflammation, and tumors, along with antiplatelet and antioxidant activities [11–13]. According to the studies, higher flavonoids and proanthocyanidin intake led to 44% and 40% lower risks for oral and laryngeal cancers, respectively. Moreover, a one-third reduction in the incidence of colon cancers was reported, along with reduced rates of breast and renal, as well as ovarian cancers. According to the above, flavonoids have anticancer potentials [14, 15].

Figure 1 shows rutin (quercetin rutinoside) as flavonoid quercetin glycoside. Researchers have found different advantages for rutin, such as inhibiting aggregation of platelet, anti-inflammation, antioxidant, and decreasing fat as well as cholesterol in the blood [16, 17]. According to a study, rutin was capable of exerting considerable and possible positive impacts on reducing precancerous complications along with triggering apoptotic conditions in cancers associated with the large intestine [18].

The science of nanotechnology is about synthesizing particles at nanoscale size ranging from 1 to 100 nm, leading to a significant surface increase (in terms of the area and atoms), as well as nanoparticles' physical and chemical properties (being bioavailable and stable) compared to the native state [19]. Therefore, it is possible to apply this technology in various areas, including biomedicine and pharmaceuticals. The nanoparticle form of phytochemicals is highly soluble and considerably efficient in cellular uptake while showing improved adsorption and requiring lower dosages. It can also target the desired tissues better and has great efficiency in treatment compared to the native state [13, 20–22].

The aim of this study was the preparation of rutin nanoparticles (RNs) with a view to improving its anticancer effect compared with rutin on the HN5 head and neck squamous cell carcinoma cell line by revealing the mechanisms of the cytotoxic effect.

## 2. Materials and Methods

**2.1. Preparation of Rutin Nanocrystals.** RNs were prepared by the ultrasonication method and solvent evaporation with rotary. Briefly, rutin (Sigma-Aldrich, Germany) was dissolved in ethanol (Merck, Germany) and hexane (Merck, Germany) was quickly added to it to achieve 50 mg/mL solution. The ethanol/hexane ratio was 25/75 by volume. The solution was then placed under ultrasonic conditions (AZ, Taiwan) with an ultrasonic source at a frequency of 50 kHz. Tween 80 (2% by weight) was used as a surfactant. The mixture was then mixed at 1000 rpm for 30 minutes. The resulting solution was placed on a rotary, and the solvent was evaporated. The resulting yellow powder was collected as rutin nanoparticles and stored at  $-20^{\circ}\text{C}$ .

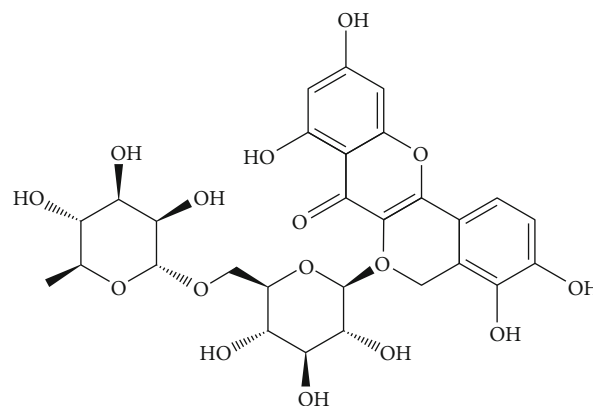


FIGURE 1: The chemical structure of rutin.

### 2.2. Characterization Evaluations

**2.2.1. Particle Size.** Dynamic Light Scattering (DLS) technique (Malvern, United Kingdom) was applied for the determination of the particle size RNs at  $25^{\circ}\text{C}$ .

**2.2.2. Scanning Electron Microscopy.** An SEM instrument (SEM, TESCAN, Warrendale, PA) was utilized for observing the morphology of the prepared RNs. For this, the powder of the nanoparticles was placed on stubs and then coated with a gold layer.

**2.2.3. Fourier Transform Infrared Spectroscopy (FTIR) and X-Ray Diffraction (XRD).** A FTIR instrument (Shimadzu 8400S, Japan) was used for detecting the FTIR spectra of the samples. The potassium bromide (IR grade) was mixed with the RNs and compressed. Besides, XRD of the samples was detected by an X-ray diffractometer (Philips TW 1710 diffractometer) with a scan rate of  $0.04^{\circ}/\text{min}$ , and the  $2\theta$  angle ranged from  $10^{\circ}$  to  $60^{\circ}$ .

**2.2.4. Cell Culture.** The HN5 SCC cell line and Human gingiva fibroblast (HGF1-PI 1) were purchased from the Pasture Institute of Iran. The HN5 and HGF1-PI1 cells were cultured in DMEM (Gibco, Germany) culture medium supplemented with 10% fetal bovine serum (FBS; Gibco, Germany), 100 U/mL streptomycin, and 100 U/mL penicillin and incubated at  $37^{\circ}\text{C}$  and 5%  $\text{CO}_2$ . Rutin trihydrate was obtained as 99% pure powder (Sigma-Aldrich, St. Louis, MO, USA).

**2.2.5. The MTT Assay.** The cytotoxic influences of rutin with different concentrations (0–2000  $\mu\text{M}$ ) and RNs (0–250  $\mu\text{M}$ ) on HN5 were evaluated via the MTT assay. The HGF1-PI1 cells as normal oral cells were treated by RNs. Both cell lines were seeded on a 96-well plate at a concentration of  $5 \times 10^3$  cells per well in DMEM supplemented with 10% FBS. Rutin (dissolved in 0.5% dimethyl sulfoxide) and RNs were added to both cell lines and incubated at  $37^{\circ}\text{C}$  and 5%  $\text{CO}_2$  for 24 and 48 hours. After, the cells were washed with phosphate-buffered saline (PBS) and then, 200  $\mu\text{L}$  of the culture medium comprising 0.5 mg/mL MTT was added to the cells, and plates were incubated at  $37^{\circ}\text{C}$  and 5%  $\text{CO}_2$  for four hours. Then, the MTT solution was changed with 200  $\mu\text{L}$

TABLE 1: The primers utilized in real-time RT-PCR.

Gene name	Sequences (5'-3')	Annealing temperature	Product size (bp)
<i>GAPDH</i> (NCBI accession number NM_002046.7)	F: AGCCACATCGCTCAGACAC R: GCCCAATACGACCAAATCC	60	66
<i>Bcl2</i> (NCBI accession number NM_000633.3)	F: CCTGTGGATGACTGAGTACC R: GAGACAGCCAGGAGAAATCA	55	128
<i>Bax</i> (NCBI accession number NM_138764.5)	F: TTTGCTTCAGGGTTTCATCCA R: CTCCATGTTACTGTCCAGTTCGT	55	151
<i>Caspase 8</i> (NCBI accession number NM_001372051.1)	F: TCCAAATGCCAAACTGGATGA R: TCCCAGGATGACCCTCTTCT	60	75
<i>Caspase 9</i> (NCBI accession number NM_001229.5)	F: CCAGAGATTTCGCAAACCAGAGG R: GAGCACCGACATCACCAAATCC	60	88

of DMSO and purple formazan crystals were dissolved and read at 570 nm by means of a spectrophotometric microplate reader (BioTek, EL ×800. USA). The cell viability percentage was calculated via the formula below:

$$\text{Cell viability (\%)} = \frac{\text{OD test} - \text{OD blank}}{\text{OD control} - \text{OD blank}} \times 100. \quad (1)$$

**2.2.6. RNA Extraction.** The concentration of rutin nanocrystals for evaluation of gene expression was the  $IC_{50}$  in 24 h. The RiboEx reagent (GeneAll Biotechnology Company, South Korea) was used for RNA extraction according to the instructions of the manufacturer. The extracted RNA was quantified using NanoDrop (Thermo Fisher Scientific, MA, USA). This process provides OD at 260 nm and 280 nm, and the ratio of OD at 260/280 nm wavelength must be about 1.8 to 2.

**2.2.7. cDNA Synthesis.** For synthesis of cDNA, 50 ng/ $\mu$ L concentration of each RNA sample was prepared, 10  $\mu$ L of which was reverse transcribed by means of a FIREScript® RT Complete Oligo-(dT) cDNA synthesis kit (Solis Bio-Dyne, Tartu, Estonia) according to the instructions of the kit manufacturer.

**2.2.8. Real-Time PCR.** qRT-PCR was performed in a Light-Cycler® 96 device (Roche Applied Science, USA) by means of a HOT FIREPol® EvaGreen® qPCR mix kit (Solis Bio-Dyne, Estonia). EvaGreen fluorescent dye binds to double-strand DNA and emits fluorescent light quantifiable by the real-time device. The amplification reactions were in a total reaction volume of 20  $\mu$ L containing the gene-specific primers (10 pmol for each), 1  $\mu$ L of cDNA (1000 ng/ $\mu$ L), and PCR master mix. Table 1 shows the characteristics of the primers utilized in real-time RT-PCR.

The following situations were used for the PCR reactions: 95°C for 12 min for an initial incubation step, followed by 40 cycles of amplification, each cycle comprising of a denaturation step at 95°C for 10 s, an annealing step at 55-60°C for 10 s depending on the primer temperature achieved by a gradient PCR test, and an extension step at 72°C for 10 s. In order to verify the amplicon specificity, the melting curve analysis was also considered. The comparative expression level of genes was calculated via the standard  $2^{-\Delta\Delta Ct}$

using the GAPDH as housekeeping gene for normalization, where Ct denotes the crossing threshold value calculated.

**2.2.9. Statistical Analysis.** Two-way ANOVA was used to evaluate the effect of concentration of rutin and RNs and exposure time on the cell's viability. One-way ANOVA was utilized to evaluate the RN's effect on tested genes, and the significance level of  $p < 0.05$  was considered.

### 3. Results

**3.1. Characterization of Rutin Nanocrystals.** The prepared RNs showed a mean particle size of  $75 \pm 0.16$  nm. Besides, the SEM results (Figure 2(a)) presented that the RNs had aggregated quasispherical, uniform small particles (Figure 2(b)).

The prepared RNs exhibited peak intensities suggesting its crystalline state (Figure 2(c)). The chemical composition of RNs was evaluated by FTIR spectra, and it could be seen that there were no noticeable differences between the absorption bands of RNs and the bulk rutin in the whole area of absorption bands (Figure 2(d)).

**3.2. The Cytotoxicity of Rutin and RNs.** In order to assess the cytotoxicity of rutin and RNs, cells were treated with several concentrations of rutin and RNs and their viability was assessed by MTT assay. Rutin did not display a significant cytotoxic effect on HN5 cells to 2000  $\mu$ M (Figure 3(a)), but RNs decreased the viability of the cells in a time- and concentration-dependent manner. The  $IC_{50}$  of RNs was calculated based on survival percentage for logarithmic concentration.  $IC_{50}$  values of RNs were 30.51  $\mu$ M and 27.34  $\mu$ M in 24 and 48 h incubation times, respectively ( $p < 0.05$ ) (Figure 3(b)). There was no significant change in the result of HGF1-PII treated by RNs after 24 h and 48 h (Figure 3(c)).

**3.3. The Expression Level of Bax and Bcl-2 Genes and Ratio of Bax/Bcl-2.** The results of real-time RT-PCR technique displayed that *Bax* mRNA level was showed a slightly and statistically not significant reduction in rutin- and RN-treated cells (Figure 4(a)). The mRNA expression level of *Bcl-2* was significantly decreased in both rutin- and RN-treated cells ( $p < 0.05$ ; Figure 4(b)). *Bax/Bcl-2* ratio is an important indicator in susceptibility of cells to apoptosis.

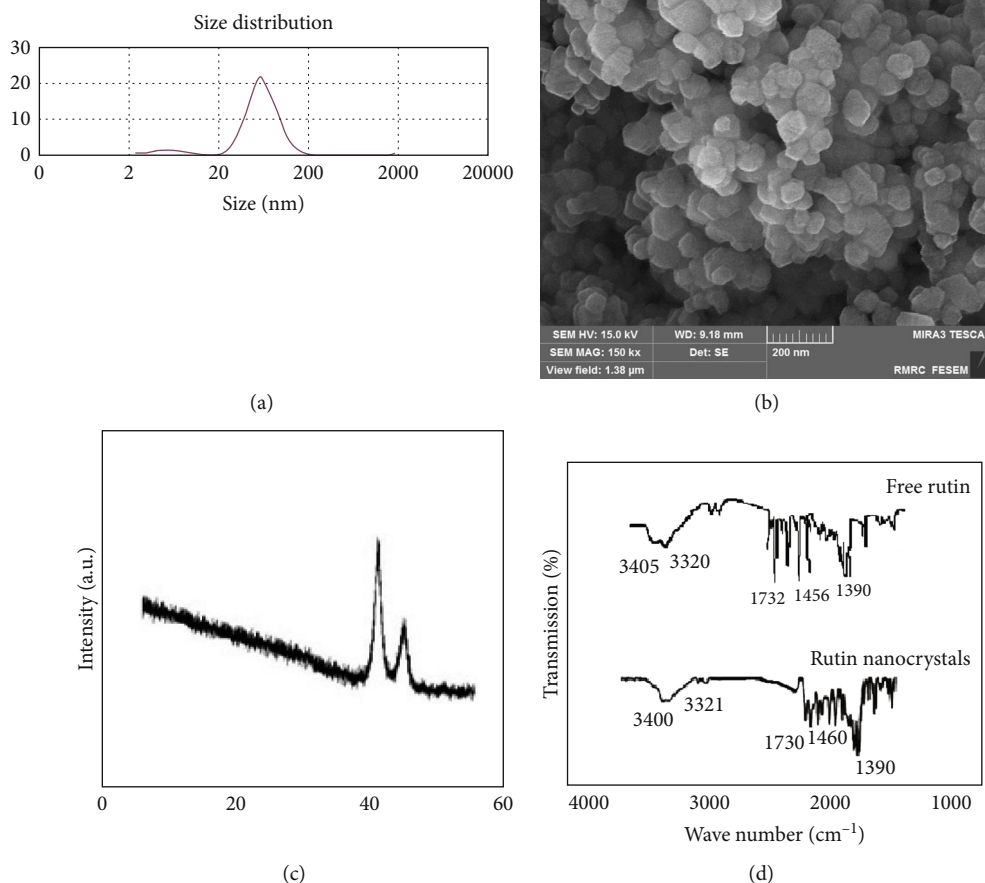


FIGURE 2: Physicochemical characterization of the prepared rutin nanocrystals: (a) distribution of particle size, (b) SEM image, (c) XRD pattern, and (d) FTIR peak for free rutin and rutin nanocrystals.

Our results displayed a significant increase in the ratio of *Bax/Bcl-2* in RN-treated cells ( $p < 0.05$ ; Figure 4(c)).

**3.4. The Expression Level of Caspase-8 and -9.** The results show a delicate change in the mRNA expression level of *caspase-8* that is not statistically significant in rutin- and RN-treated cells (Figure 5(a)). Similarly, the gene expression level of *caspase-9* was gently increased in RN-treated cells, even though that is not significant (Figure 5(b)).

## 4. Discussion

Nanotechnology and nanomedical concepts represent the possibilities for developing rutin delivery systems at the nanoscale. We prepared RNs to enhance efficiency and investigate their ability to prevent the proliferation of HN-5 cells *in vitro*. The prepared RNs had a mean particle size of  $75 \pm 0.16$  nm and aggregated quasispherical, uniform small particles (Figures 2(a) and 2(b)). The type of applied preparation method has a great impact on the morphology of the resulting nanoparticles. Thorat and Dalvi showed that

in the presence of an ultrasonic system, the resulting nanoparticles have a predominantly aggregate quasispherical morphology [23]. The prepared RNs exhibited the lower peak intensities comparing to the bulk rutin, suggesting the smaller sizes and lower crystallinity that was consistent with our SEM results (Figure 2(c)).

The FTIR study (Figure 2(d)) exhibited absorptions for stretching of C=O groups;  $1730 \text{ cm}^{-1}$  for the ester group,  $1460 \text{ cm}^{-1}$  for the ketone group, and  $1390 \text{ cm}^{-1}$  for the ether group. Besides, a broad peak at  $3400 \text{ cm}^{-1}$  is related to the stretching vibration of the OH group [24–26]. There were no noticeable differences between the absorption bands of RNs and the free rutin in the whole area of absorption bands. Then, the results showed that the sonication method did not show any effect on the chemical compositions of rutin.

When examined for its capability to suppress the growth of cancer cells, we found that cytotoxicity of RNs was at least 100 times more than free rutin.

It may be clarified that rutin nanocrystals are well soluble in water. The good solubility of nanocrystals decreases

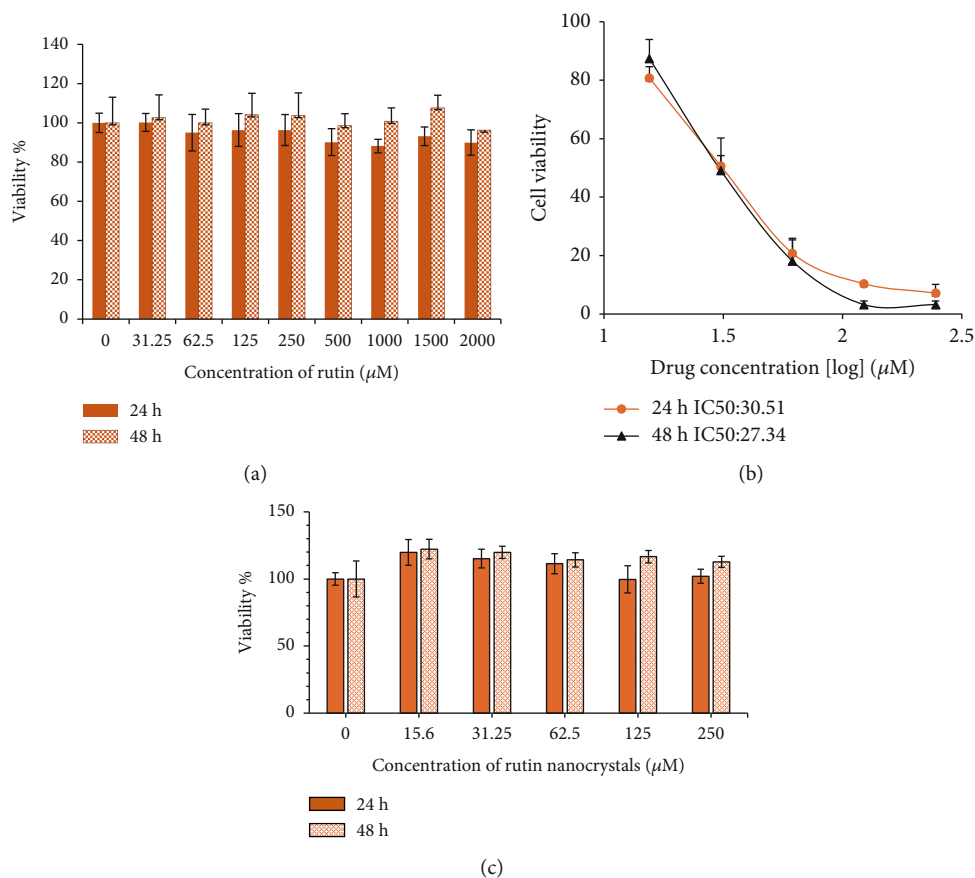


FIGURE 3: The cytotoxicity of rutin and rutin nanocrystals by MTT assay: (a) the cytotoxic effect of rutin on HN5 cells in 24 and 48 h, (b) the cytotoxic effect of RNs on HN5 cells with the calculation of IC50 in 24 and 48 h, and (c) the cytotoxic effect of RNs on HGF1-PI1 in 24 h and 48 h.

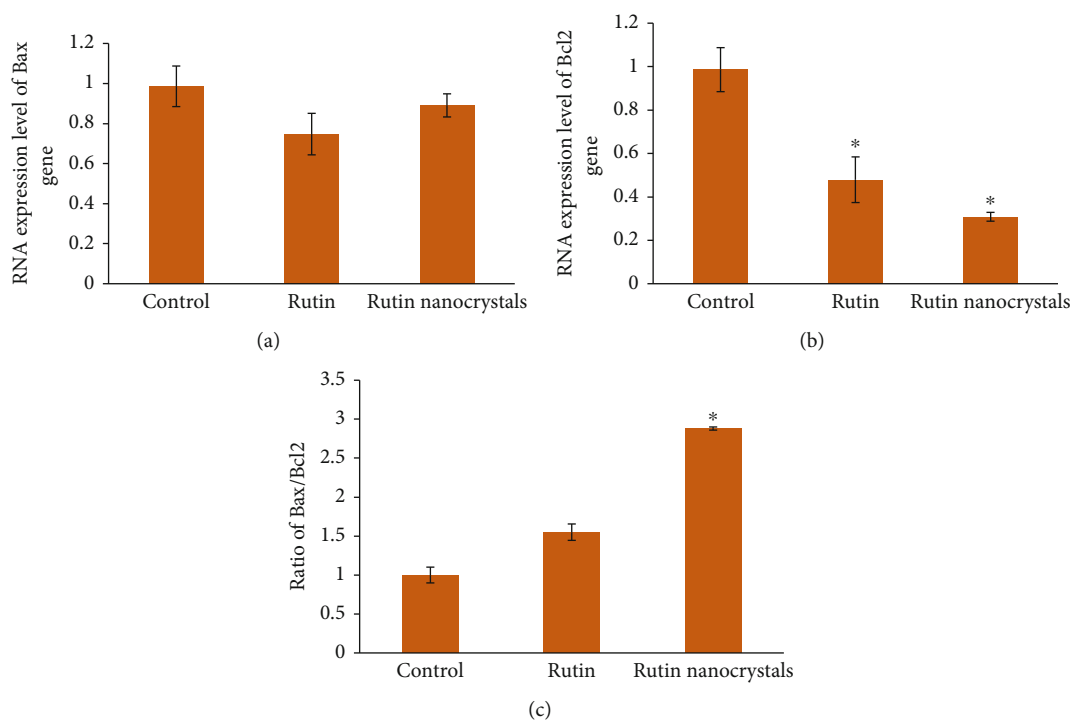


FIGURE 4: Expression levels of *Bax* and *Bcl-2* genes and *Bax/Bcl-2* ratio of rutin- and RN-treated cells compared with control.

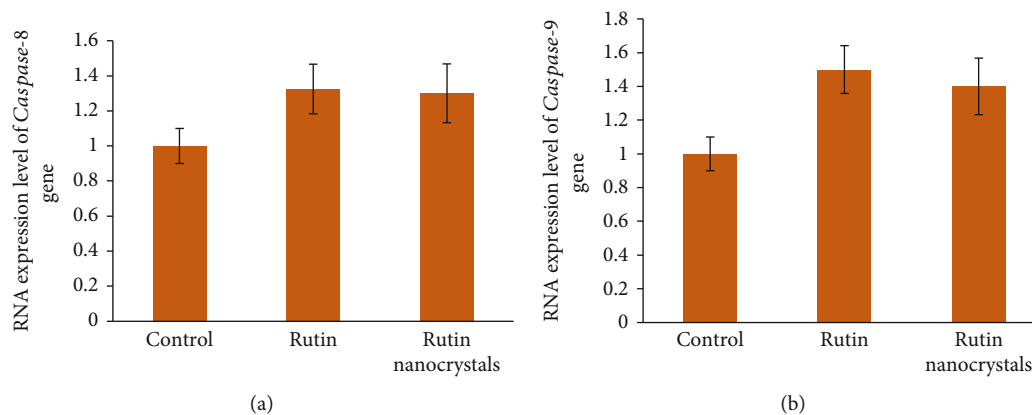


FIGURE 5: Expression levels of *Caspase-8* and *-9* of rutin- and RN-treated cells compared with control.

the energy barrier and consequently increases the intermembrane transfer rate. Then, the absorption of rutin in nanoform into cells is higher than that of bulk rutin [27]. Hoai et al. also reported this explanation for their rutin-loaded polymeric nanoparticles [27]. Besides, it has shown that particle size and shape eventually control the successful uptake of nanoparticles into cells and have an important role for initial internalization into cells [28]. The prepared RNs in this study had a mean particle size of  $75 \pm 0.16$  nm and a quasospherical shape. Some reports show that the spherical nanoparticles reveal the fastest internalization rate, compared to the other morphologies [29]. Based on free energy rules, the spherical nanoparticles need to overcome a minimal membrane bending energy barrier, compared with the nonspherical particles [29]. It has also shown that small particles (between 25 and 100 nm) are likely to be ingested by tip-first uptake mode, facing the membrane with the lowest curvature side [28, 30].

Apoptotic conditions are triggered by cytotoxic agents as the death signaling pathways are initiated by insensitive target cells [31]. The death receptor systems are simultaneously or consequently activated due to activation of apoptotic conditions by chemotherapy, while the mitochondrial functions, as well as caspases proteolytic processing, are also disturbed [32]. Therefore, it is possible that the cellular death pathway occurs in different locations; nevertheless, there is no complete information on the exact molecular mechanisms involved in every special medicine and each specific target cell. The present work provided reports on the alterations in *Bcl-2* (antiapoptotic) and *Bax* (proapoptotic) genes' expression and *Bax/Bcl-2* ratio as well as *caspase-8* and *-9* expression levels after stimulating apoptotic state through RNs in HN-5 cells.

For assessment of cytotoxicity induced by rutin and RNs, the MTT assay was applied. Rutin did not show any significant cytotoxic effect on HN5 cells to  $2000 \mu\text{M}$ , but RNs displayed cytotoxic effect with an  $\text{IC}_{50}$  of  $30.51 \mu\text{M}$  and  $27.34 \mu\text{M}$  in 24 and 48 h incubation times, respectively ( $p < 0.05$ ).

The death or survival of the cells is mainly regulated by the *Bcl-2* family members. Chemotherapy controls partly the expression of different *Bcl-2* family members in cancer-

ous cells. The proteins of this family contribute significantly to the apoptotic conditions through activation (*Bax*) or inhibition (*Bcl-2*) [33, 34].

Three different parameters were examined in the present work including *Bax* and *Bcl-2* gene absolute expression levels, along with their ratios in vitro. The ratios of *Bax* to *Bcl-2* help determine the cell destiny compared to their absolute concentrations [35]. A considerable percentage of *Bax* to *Bcl-2* ratios is originated when HN-5 is treated by RNs ( $p < 0.05$ ). Therefore, according to the observations in the present work and similar studies, imbalanced expression of *Bax* and *Bcl-2* overtreating by RNs seems to contribute significantly to apoptotic conditions induced by RNs [36].

The presence of a special apoptotic mechanism in the treatment of HN-5 cells by RNs is supported in this study, since the increase in the ratio of *Bax* to *Bcl-2* makes cells less viable while the apoptotic state increases. Furthermore, the expression of *Bax* seems to activate caspases and subsequent apoptotic conditions [37, 38].

## 5. Conclusion

RNs can show a minimum of 100 times higher potential in suppressing the development of cancerous cells compared to bulk rutin. Based on the obtained data, increasing the ratio of *Bax* to *Bcl-2* contributes significantly to HN-5 cell apoptotic state triggered by RNs; nevertheless, more research is required for validation of these results. The present findings can highlight the unharnessed capability of RNs as adjuvants to be applied in the treatment of different cancerous cells.

## Data Availability

The data used to support the findings of this study are included within the article.

## Conflicts of Interest

No conflict of interest is declared by the authors.

## Acknowledgments

The present paper was derived from a thesis provided at the Faculty of Dentistry, Tabriz University of Medical Sciences (number 66412). The authors would like to appreciate the financial supports given by the Vice-Chancellor for Research at Tabriz University of Medical Sciences.

## References

- [1] A. J. Abassi, A. Mohamadnia, S. A. Parhiz, N. Azizi Moghadam, and N. Bahrami, "Cytotoxic effect of thiabendazole on HN5 head and neck squamous cell carcinoma cell line," *Journal of Dentistry*, vol. 18, no. 3, pp. 219–226, 2017.
- [2] C. Llewellyn, N. Johnson, and K. Warnakulasuriya, "Risk factors for squamous cell carcinoma of the oral cavity in young people – a comprehensive literature review," *Oral Oncology*, vol. 37, no. 5, pp. 401–418, 2001.
- [3] S. Silverman Jr., "Demographics and occurrence of oral and pharyngeal cancers: the outcomes, the trends, the challenge," *The Journal of the American Dental Association*, vol. 132, pp. 7S–11S, 2001.
- [4] S. Silverman Jr. and M. Gorsky, "Epidemiologic and Demographic Update in Oral Cancer: California and National Data–1973 to 1985," *The Journal of the American Dental Association*, vol. 120, no. 5, pp. 495–499, 1990.
- [5] P. A. Swango, "Cancers of the oral cavity and pharynx in the United States: an epidemiologic overview," *Journal of Public Health Dentistry*, vol. 56, no. 6, pp. 309–318, 1996.
- [6] M. Mohseni, N. Samadi, P. Ghanbari et al., "Co-treatment by docetaxel and vinblastine breaks down P-glycoprotein mediated chemo-resistance," *Iranian Journal of Basic Medical Sciences*, vol. 19, no. 3, pp. 300–309, 2016.
- [7] S.-R. Lin, Y.-S. Fu, M.-J. Tsai, H. Cheng, and C.-F. Weng, "Natural compounds from herbs that can potentially execute as autophagy inducers for cancer therapy," *International Journal of Molecular Sciences*, vol. 18, no. 7, p. 1412, 2017.
- [8] S. Sharifi, F. A. Moghaddam, A. Abedi et al., "Phytochemicals impact on osteogenic differentiation of mesenchymal stem cells," *BioFactors*, vol. 46, no. 6, pp. 874–893, 2020.
- [9] N. Samadi, P. Ghanbari, M. Mohseni et al., "Combination therapy increases the efficacy of docetaxel, vinblastine and tamoxifen in cancer cells," *Journal of Cancer Research and Therapeutics*, vol. 10, no. 3, pp. 715–721, 2014.
- [10] M. Armat, T. Oghabi Bakhshaesh, M. Sabzichi et al., "The role of Six1 signaling in paclitaxel-dependent apoptosis in MCF-7 cell line," *Bosnian Journal of Basic Medical Sciences*, vol. 16, no. 1, pp. 28–34, 2016.
- [11] X. Montané, O. Kowalczyk, B. Reig-Vano et al., "Current perspectives of the applications of polyphenols and flavonoids in cancer therapy," *Molecules*, vol. 25, no. 15, p. 3342, 2020.
- [12] I. Sheikh, V. Sharma, H. S. Tuli et al., "Cancer chemoprevention by flavonoids, dietary polyphenols and terpenoids," *Biointerface Research in Applied Chemistry*, vol. 11, no. 1, pp. 8502–8537, 2021.
- [13] R. Negahdari, S. Bohlouli, S. Sharifi et al., "Therapeutic benefits of rutin and its nanoformulations," *Phytotherapy Research*, vol. 35, no. 4, pp. 1719–1738, 2021.
- [14] D. F. Romagnolo and O. I. Selmin, "Flavonoids and cancer prevention: a review of the evidence," *Journal of nutrition in gerontology and geriatrics*, vol. 31, no. 3, pp. 206–238, 2012.
- [15] D. Maggioni, L. Biffi, G. Nicolini, and W. Garavello, "Flavonoids in oral cancer prevention and therapy," *European Journal of Cancer Prevention*, vol. 24, no. 6, pp. 517–528, 2015.
- [16] C. H. Jung, J. Y. Lee, C. H. Cho, and C. J. Kim, "Anti-asthmatic action of quercetin and rutin in conscious guinea-pigs challenged with aerosolized ovalbumin," *Archives of Pharmacol Research*, vol. 30, no. 12, pp. 1599–1607, 2007.
- [17] A. Imani, N. Maleki, S. Bohlouli, M. Kouhsoltani, S. Sharifi, and S. Maleki Dizaj, "Molecular mechanisms of anticancer effect of rutin," *Phytotherapy Research*, vol. 35, no. 5, pp. 2500–2513, 2021.
- [18] S. R. Volate, D. M. Davenport, S. J. Muga, and M. J. Wargovich, "Modulation of aberrant crypt foci and apoptosis by dietary herbal supplements (quercetin, curcumin, silymarin, ginseng and rutin)," *Carcinogenesis*, vol. 26, no. 8, pp. 1450–1456, 2005.
- [19] Y. J. Chen, B. S. Inbaraj, Y. S. Pu, and B. H. Chen, "Development of lycopene micelle and lycopene chylomicron and a comparison of bioavailability," *Nanotechnology*, vol. 25, no. 15, article 155102, 2014.
- [20] C. Wen, Y. Zhou, C. Zhou et al., "Enhanced radiosensitization effect of curcumin delivered by PVP-PCL nanoparticle in lung cancer," *Journal of Nanomaterials*, vol. 2017, Article ID 9625909, 8 pages, 2017.
- [21] P. Anand, A. B. Kunnumakkara, R. A. Newman, and B. B. Aggarwal, "Bioavailability of curcumin: problems and promises," *Molecular Pharmaceutics*, vol. 4, no. 6, pp. 807–818, 2007.
- [22] M. Fathi, E. D. Abdolahinia, J. Barar, and Y. J. N. Omid, "Smart stimuli-responsive biopolymeric nanomedicines for targeted therapy of solid tumors," *Nanomedicine*, vol. 15, no. 22, pp. 2171–2200, 2020.
- [23] A. A. Thorat and S. V. Dalvi, "Particle formation pathways and polymorphism of curcumin induced by ultrasound and additives during liquid antisolvent precipitation," *CrystEngComm*, vol. 16, no. 48, pp. 11102–11114, 2014.
- [24] S. Sun, Q. Zhou, X. Liang, and X. Yang, "Quantitative analysis of rutin and vitamin C by NIR FTIR," *Guang pu xue yu Guang pu fen xi = Guang pu*, vol. 20, no. 4, pp. 474–476, 2000.
- [25] Z. Hoopesand, S. Ghanbarzadeh, and H. Hamishehkar, "Preparation and characterization of rutin-loaded nanophytosomes," *Pharmaceutical Sciences*, vol. 21, no. 3, pp. 145–151, 2015.
- [26] N. A. Fathy, S. T. El-Wakeel, and R. R. Abd El-Latif, "Biosorption and desorption studies on chromium(VI) by novel biosorbents of raw rutin and rutin resin," *Journal of Environmental Chemical Engineering*, vol. 3, no. 2, pp. 1137–1145, 2015.
- [27] T. T. Hoai, P. T. Yen, T. T. B. Dao et al., "Evaluation of the cytotoxic effect of rutin prenanoemulsion in lung and colon cancer cell lines," *Journal of Nanomaterials*, vol. 2020, Article ID 8867669, 11 pages, 2020.
- [28] E. Blanco, H. Shen, and M. Ferrari, "Principles of nanoparticle design for overcoming biological barriers to drug delivery," *Nature Biotechnology*, vol. 33, no. 9, pp. 941–951, 2015.
- [29] Y. Li, M. Kröger, and W. K. Liu, "Shape effect in cellular uptake of PEGylated nanoparticles: comparison between sphere, rod, cube and disk," *Nanoscale*, vol. 7, no. 40, pp. 16631–16646, 2015.
- [30] M. V. Baranov, M. Kumar, S. Sacanna, S. Thutupalli, and G. Van Den Bogaart, "Modulation of immune responses by

- particle size and shape," *Frontiers in Immunology*, vol. 11, p. 3854, 2021.
- [31] D. E. Fisher, "Apoptosis in cancer therapy: crossing the threshold," *Cell*, vol. 78, no. 4, pp. 539–542, 1994.
- [32] K.-M. Debatin, *Cytotoxic Drugs, Programmed Cell Death, and the Immune System: Defining New Roles in an Old Play*, vol. 89, no. 11, 1997 Oxford University Press, 1997.
- [33] D. R. Green and J. C. Reed, "Mitochondria and apoptosis," *science*, vol. 281, no. 5381, pp. 1309–1312, 1998.
- [34] L. Rao and E. White, "Bcl-2 and the ICE family of apoptotic regulators: making a connection," *Current Opinion in Genetics & Development*, vol. 7, no. 1, pp. 52–58, 1997.
- [35] A. Gross, "BCL-2 proteins: regulators of the mitochondrial apoptotic program," *IUBMB Life*, vol. 52, no. 3-5, pp. 231–236, 2001.
- [36] H. Huynh, "Induction of apoptosis in rat ventral prostate by finasteride is associated with alteration in MAP kinase pathways and Bcl-2 related family of proteins," *International Journal of Oncology*, vol. 20, no. 6, pp. 1297–1303, 2002.
- [37] T. Rossé, R. Olivier, L. Monney et al., "Bcl-2 prolongs cell survival after Bax-induced release of cytochrome *c*," *Nature*, vol. 391, no. 6666, pp. 496–499, 1998.
- [38] S. Kagawa, S. Pearson, L. Ji et al., "A binary adenoviral vector system for expressing high levels of the proapoptotic gene *bax*," *Gene Therapy*, vol. 7, no. 1, pp. 75–79, 2000.